

PAPER

Simulation of the long wavelength sound-wave CT using prior information

Juzhong Dong, Yuukou Horita and Tadakuni Murai

Faculty of Engineering, Toyama University,

3190 Gofuku, Toyama, 930-8555 Japan

e-mail: dongiz@cslab.eng.toyama-u.ac.jp

(Received 17 June 2000, Accepted for publication 6 April 2001)

Abstract: A simulation study about the CT technique employing a stationary sound wave with long wavelength is presented. The CT is an inverse and nonlinear problem, so that an iterative approach is inevitable. That is, starting an assumed density distribution, the field calculation is repeatedly made until a true density distribution is achieved. An inhomogeneous domain is divided into subregions in which the density is assumed to be constant. The Finite Element Method is used for calculating the acoustic field under the given particle velocity driving source and the Newton-Raphson method is used to update the initial density distribution by minimizing the scalar error between computed and measured field values. To cope with the ill-condition which essentially exist in the inverse problem, three kinds of methods are used comparatively to solve this problem. For getting a more exact reconstruction, a new algorithm employing prior information is proposed. The simulation results show that the proposed algorithm can reconstruct satisfactorily the density distribution image of the model by the proper selection of driving position and its frequency.

Keywords: Sound-wave CT, Finite element method, Newton-Raphson method, Prior information, Regularization method

PACS number: 43.60.Pt

1. INTRODUCTION

Ultrasonic CT is useful for medical purpose. However, because biological tissue is inhomogeneous and sound wave suffers the influences of refraction and dispersion, there will exist a distorted tomography or artifact when the sound wave is assumed to travel in straight line and the acoustic parameter distribution of the object is estimated by using the time difference between the incident sound wave and the echo sound wave [1,2]. On the other hand, when the sound wave has a higher frequency so that its travel is more approximate to a straight line, the decay of the sound wave becomes great.

Another type of interesting imaging technique is the CT that takes the refraction into consideration and is basically the same approach as microwave tomography [3,4]. As the result, a stationary long wavelength sound wave CT was proposed to solve the object identification problem [1].

In this paper, the acoustic parameter reconstruction technique is investigated by numerical simulation. A model including two kinds of media is employed as a approximation of the biological tissue, and then the finite element method is employed to solve the acoustic field of the model for the long sound wavelength so that the refraction and

dispersion of the sound wave travel can be taken into consideration. Based on the difference of the boundary measurement between the actual model and the assumed model under the same stationary incident sound waves, the acoustic parameter distribution image of the model is reconstructed by the use of the Newton-Raphson method and one of the regularization methods (such as the Truncated Singular Value Decomposition (TSVD) method, Tikhonov method or Marquardt method). To get a more precise image, an algorithm employing prior information is proposed. On the basis of above, the effect of the driving and observing position, the measurement noise and driving frequency on the reconstruction are investigated.

2. MODEL AND SOLUTION OF THE STATIONARY ACOUSTIC FIELD

2.1. Model and Problem

To simplify the task and be representative, a two-dimensional ellipse model as shown in Fig. 1 is selected. The white part of it is assumed to represent the lung (density $\rho_1 = 400.0 \text{ kg/m}^3$, sound speed $c_1 = 658 \text{ m/s}$), and the black part to represent the tissue around the lung ($\rho_2 = 1,070.0 \text{ kg/m}^3$, $c_2 = 1,566 \text{ m/s}$). The outside of the ellipse model is air region ($\rho_3 = 1.2 \text{ kg/m}^3$, $c_3 = 340 \text{ m/s}$).

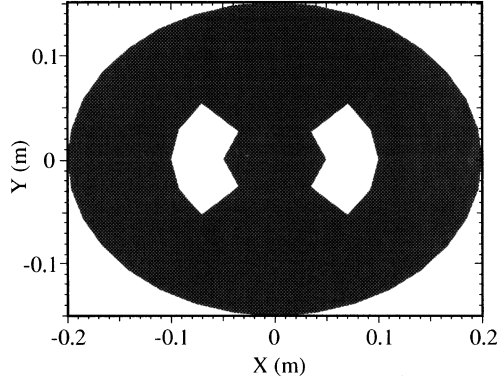


Fig. 1 Two medium model examined. The white and black parts indicate the image view of the acoustic parameter distribution.

The aim of our sound wave CT is to reconstruct the acoustic parameter distribution within the ellipse model. When a constant particle velocity sound wave is excited toward a part of boundary of the model, a measurement of sound pressures is made at the other part of the boundary of the ellipse model. Then, some algorithms are used for reconstructing the image of the acoustic parameter distribution of the ellipse model.

2.2. Solution of the Stationary Acoustic Field

The model described above is inhomogeneous. The governing equation of its acoustic field can be written as [5]

$$\nabla \cdot \left(\frac{1}{\rho} \nabla p \right) - \frac{\partial}{\partial t} \left(\frac{1}{\rho c^2} \frac{\partial p}{\partial t} \right) = 0, \quad (1)$$

$$\frac{\partial p}{\partial n} = \hat{q} \quad (\text{on the } \Gamma_d), \quad (2)$$

where p is the sound pressure, ρ is the medium density, c is the sound speed, and t is time, Γ_d is the boundary driven, $\partial/\partial n$ is normal derivative to the boundary and symbol \hat{q} indicates the prescribed value.

Because the sound wave used here has a relatively long wavelength, the finite element method is suitable to solve the acoustic field of the model. The finite element mesh with 128 triangular elements is shown in Fig. 2.

The whole field is divided into finite region Ω_F and infinite region Ω_I (air region) by its boundary Γ . In the finite region, density and sound speed within each element are assumed to be constant, and the discretized equation derived by the usual finite element method can be written as

$$\begin{bmatrix} [Y]_{FF} & [Y]_{FI} \\ [Y]_{IF} & [Y]_{II} \end{bmatrix} \begin{bmatrix} P_F \\ P_I \end{bmatrix} = \begin{bmatrix} W_F \\ W_I \end{bmatrix}, \quad (3)$$

here

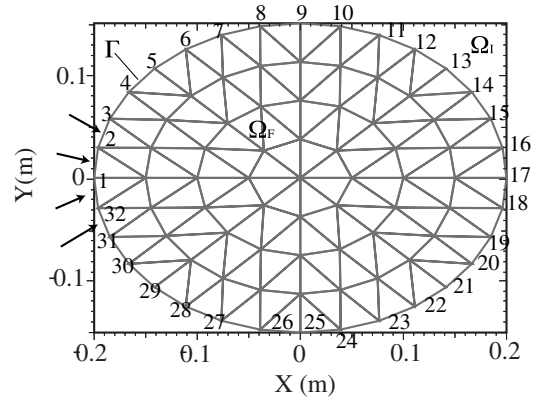


Fig. 2 Mesh used in FEM. The integer indicates the node number.

$$\begin{bmatrix} [Y]_{FF} & [Y]_{FI} \\ [Y]_{IF} & [Y]_{II} \end{bmatrix} = [\hat{M} - k^2 K], \quad (4)$$

where $[Y]$ is the coefficient matrix, k is the wave number, \hat{M} is the inertance matrix, K is the elastance matrix, $[P_F P_I]^T$ is the vector of sound pressure at nodes and $[W_F W_I]^T$ is the 'force vector'. Subscripts F and I indicate the finite region and the infinite region respectively. On the other hand, in the infinite region, the infinite element based on the hybrid formation [6] is used. If the equations of two regions are combined, the sound pressures at each node of the mesh can be obtained. The whole equation can be expressed as follows:

$$\begin{bmatrix} [Y]_{FF} & [Y]_{FI} \\ [Y]_{IF} & [Y]_{II} + [y]_{II} \end{bmatrix} \begin{bmatrix} P_F \\ P_I \end{bmatrix} = \begin{bmatrix} W_F \\ 0 \end{bmatrix}, \quad (5)$$

where $[y]_{II}$ is the coefficient matrix in the infinite region.

To indicate the validity of the finite element approach used in this paper, the amplitude and phase distribution of the sound pressure are shown in Fig. 3. In this case, the values of sound speed and medium density are identical to those shown in section 2.1 and first-order triangle element is used. It is found visually that the finite element approach used is suitable in this long wavelength situation.

3. INVERSE ALGORITHM

In this paper, the acoustic parameter within each element is assumed to be constant. Therefore, the aim of our inverse problem is to find the acoustic parameter of each element. To do this, the field calculation is initiated from an assumed acoustic parameter distribution until a true acoustic parameter distribution is achieved so as to minimize the cost function constructed with the "measured" and computed sound pressures on the boundary.

To obtain a stable convergence, a certain number of observation points is needed. To do this, a multi-drive mode is selected as a driving method. For example, the 3-

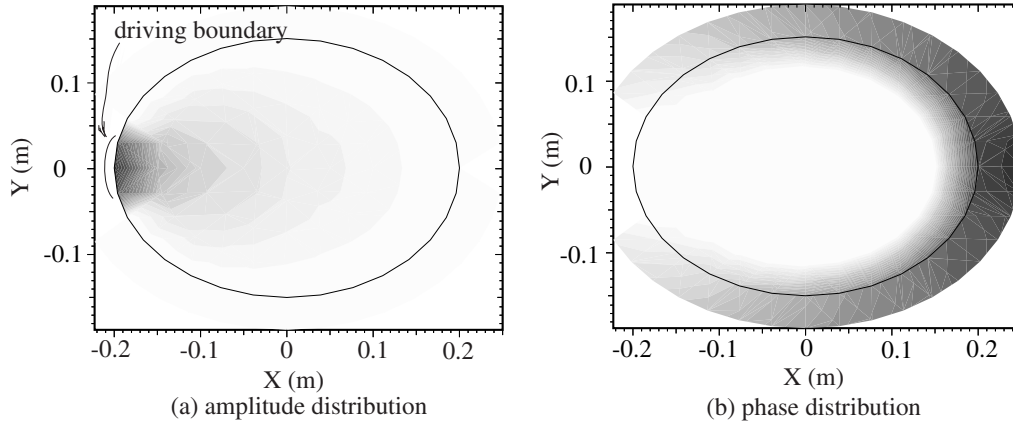


Fig. 3 Profiles of the amplitude and phase distributions of the sound pressure. The boundary connected by the nodes 31, 32, 1, 2, 3 is driven by the constant particle velocity with frequency 1,275 Hz whose wavelength is relatively longer than the size of the ellipse model. The shaded and light parts indicate the strong and weak amplitudes and phase shift.

drive mode method can be shown as follows:

Referring to Fig. 2, for the first drive, the boundary connected by the nodes 31, 32, 1, 2, 3 is driven by a constant particle velocity, and the sound pressures of the boundary nodes 4, 5, ..., 30 are measured. For the second drive, the boundary connected by the nodes 7, 8, 9, 10, 11 is driven, and the sound pressures of nodes 12, 13, ..., 5, 6 are measured. For the final drive, the boundary connected by the nodes 15, 16, 17, 18, 19 is driven, and the sound pressures of nodes 20, 21, ..., 13, 14 are measured.

Denoting the sound pressures of the boundary nodes of the actual model by $\hat{P}_{ll'}$, and denoting those of the assumed model by $P_{ll'}$, then the cost function to be minimized in the inverse problem can be selected as

$$J = \sum_{l=1}^{mc} \sum_{l'=1}^m (\hat{P}_{ll'} - P_{ll'}) (\overline{\hat{P}_{ll'} - P_{ll'}}), \quad (6)$$

where mc is the number of all drives, m is the number of measurement nodes, l denotes the drive number, l' the measurement node number, and $\overline{\hat{P}_{ll'} - P_{ll'}}$ means the conjugate complex of $\hat{P}_{ll'} - P_{ll'}$. The assumed model means the model in which the acoustic parameters distribution is assumed.

If J is small enough, the assumed distribution will be thought to be equal to the actual distribution. As the two vectors, $\hat{P}_{ll'}$ and $P_{ll'}$, are not equal generally and J also is not small enough, a correction of the assumed distribution is needed. Here, the Newton-Raphson method is selected to update the assumed distribution and its recursion equation can be expressed as

$$\rho_{k+1} = \rho_k - \delta_k M^{-1} \left(\frac{\partial J}{\partial \rho} \right)_k, \quad (7)$$

where the ρ_{k+1} denotes the $(k+1)$ th estimated distribution vector, and the ρ_k denotes the k th estimated distribution vector. M is the Hessian matrix and the δ_k is the longest

step which make the J_{k+1} as possible as less than J_k for update.

$\partial J / \partial \rho$ and the component M_{ij} of the matrix M can be given by the following equation:

$$\frac{\partial J}{\partial \rho} = \left[\frac{\partial J}{\partial \rho_1} \frac{\partial J}{\partial \rho_2} \cdots \frac{\partial J}{\partial \rho_n} \right]^T \quad (8)$$

$$= - \sum_{l=1}^{mc} \sum_{l'=1}^m \left[\frac{\partial P_{ll'}}{\partial \rho} (\overline{\hat{P}_{ll'} - P_{ll'}}) + (\hat{P}_{ll'} - P_{ll'}) \frac{\partial \overline{P_{ll'}}}{\partial \rho} \right], \quad (9)$$

$$M_{ij} = \frac{\partial^2 J}{\partial \rho_i \partial \rho_j} = \sum_{l=1}^{mc} \sum_{l'=1}^m \left[\frac{\partial P_{ll'}}{\partial \rho_i} \frac{\partial \overline{P_{ll'}}}{\partial \rho_j} + \frac{\partial P_{ll'}}{\partial \rho_j} \frac{\partial \overline{P_{ll'}}}{\partial \rho_i} \right], \quad (10)$$

where n indicates the number of elements in mesh, and ρ_i denotes the i th component of the ρ . M is a symmetrical matrix with $n \times n$ dimension. If the discretized Eq. (5) with the k th estimated distribution can be expressed by $A_k P_k = B_k$, then $\partial P_k / \partial \rho_i$ can be expressed by the following equation

$$\frac{\partial P_k}{\partial \rho_i} = -A_k^{-1} \frac{dA_k}{d\rho_i} A_k^{-1} B_k \quad (11)$$

$$= -A_k^{-1} \frac{dA_k}{d\rho_i} P_k. \quad (12)$$

A greater n means a higher resolution of the reconstruction image, but a greater n will increase the condition number of the matrix M , this is so called ill-condition. To solve the ill-condition problem, there are several regularization methods proposed before [7,8]. In this paper, the TSVD method, Tikhonov method and Marquardt method are applied comparatively to the inverse problem and a new “regularization method” using the prior information is proposed to obtain a better result.

3.1. Conventional Reconstruction Methods Examined

3.1.1. TSVD regularization method

As the condition number of the M matrix can be thought as the magnification coefficient of the error, the error in the $(\partial J / \partial \rho)_k$ will be magnified inappropriately to make the inverse problem difficult to solve when it becomes greater. The condition number of M matrix in the inverse problem above gets greater than 10^{12} . TSVD regularization method sets a limit to the condition number of M matrix by setting the singular values less than the given value to zero when the inverse matrix of M matrix is solved. As the consequence, it will have some influence on the reconstruction image due to some singular values being neglected and some information about the model being thrown away.

The matrix M in Eq. (7) can be decomposed as follows:

$$M = U \Lambda U^T, \quad (13)$$

where U is a unitary matrix whose components consist of eigenvectors of matrix M , and Λ can be expressed as follows

$$\Lambda = \begin{bmatrix} \lambda_1 & 0 & \cdots & 0 \\ 0 & \lambda_2 & \cdots & 0 \\ \vdots & \vdots & \ddots & \vdots \\ 0 & 0 & \cdots & \lambda_n \end{bmatrix} \quad \lambda_1 \geq \lambda_2 \geq \cdots \geq \lambda_n, \quad (14)$$

where λ_i ($i = 1, 2, \dots, n$) are singular values. The approximate inverse matrix M^{-1} in Eq. (7) can be given as follows:

$$M^{-1} = U \Lambda^+ U^T, \quad (15)$$

where

$$\Lambda^+ = \begin{bmatrix} \frac{1}{\lambda_1} & 0 & \cdots & 0 & \cdots \\ 0 & \frac{1}{\lambda_2} & \cdots & 0 & \cdots \\ \vdots & \vdots & \ddots & \vdots & \vdots \\ 0 & 0 & \cdots & \frac{1}{\lambda_k} & \cdots \\ \vdots & \vdots & \ddots & \vdots & 0 \end{bmatrix}. \quad (16)$$

In this case, it is important to select the parameter k properly for obtaining the reasonable solution. There are some methods for selecting the k [1,7,9], however, here k is selected so as to satisfy $\gamma/\lambda_k^2 > 10.0$, in which γ can be selected empirically or by other methods.

3.1.2. Tikhonov regularization method

Tikhonov regularization method gives a reasonable solution by adding an additional penalty item into the cost function. As the result, the approximate inverse matrix M^{-1} in Eq. (7) can be calculated as follows:

$$M^{-1} = U \Lambda^+ U^T, \quad (17)$$

$$\Lambda^+ = \begin{bmatrix} \frac{1}{\lambda_1 + \frac{\gamma}{\lambda_1}} & 0 & \cdots & 0 \\ 0 & \frac{1}{\lambda_2 + \frac{\gamma}{\lambda_2}} & \cdots & 0 \\ \vdots & \vdots & \ddots & \vdots \\ 0 & 0 & 0 & \frac{1}{\lambda_n + \frac{\gamma}{\lambda_n}} \end{bmatrix}. \quad (18)$$

In the same way as TSVD method, a proper choice of the parameter γ is important.

3.1.3. Marquardt regularization method

Yorkey [9] pointed out that discarding some small eigenvalues and its corresponding eigenvectors would discard information about the central physics parameters distribution, and Bard [10] showed that the superiority of Marquardt method is over that of the singular value decomposition method (SVD) and many other methods.

Instead of the Eq. (7), Marquardt regularization method [10] forms

$$\rho_{k+1} = \rho_k - \delta_k (M + \gamma I)^{-1} \left(\frac{\partial J}{\partial \rho} \right)_k, \quad (19)$$

in which I is a $n \times n$ identity matrix.

γ can always be chosen appropriately so as to make the $(M + \gamma I)$ to be positive definite, this guarantees that if $(\partial J / \partial \rho)_k \neq 0$, then, $J_{k+1} < J_k$ always can be achieved with a sufficiently small positive δ_k .

3.2. Combination with the Prior Information

Because there is an insufficient information in the inverse problem usually as compared with the forward problem, it is worth while thinking that the use of the prior information can focus the solution space on a less region. To this end, Jones [8] proposed a zooming method for the Optical CT which implicates that the unknown absorption coefficient is assumed to be 'blocky', i.e., a piecewise constant function with sharp edges. This approach needs a subjective judgment for deciding the regions to be zoomed and hence some reconstruction errors would be remained. Hua [11] and David [12] proposed a Tikhonov-type regularization respectively for Electrical Impedance Tomography that adds an additional penalty item into the cost function by employing the first and second difference operators, however, its implicit prior assumption is not appropriate in some cases. Vauhkonen [13,14] proposed a method which 'draws' the solution toward the prior distribution subspace by using the generalized Tikhonov regularization method with properly constructed regularization matrix, but the method needs an appropriate learning set of reconstructed parameters which can exhibit

the corresponding feature well. However, this is a difficult task.

In our case, because of the severe ill-condition and the highly nonlinear, the reconstruction can not approach to a satisfactory extent and the estimated acoustic parameters of elements of the same medium are located dispersively when the reconstruction algorithms combining Newton-Raphson method with the above regularization methods are used. It is evident that the iterative schemes are trapped in local minima of the cost function. To find the global minimum of the cost function, the random optimization methods such as Genetic Algorithm can be used. However, these optimization methods have the limitation that they usually take extensive time for convergence. Therefore, in this paper, a new reconstruction algorithm is proposed. In this approach, the conventional algorithm and a kind of modification technique based on the prior information are alternatively used. The former is used to find a local minimum of the cost function with comparatively few steps and the latter is used to “guide” the result toward the global minimum of the cost function, which takes a same role as regularization.

The basic feature of the modification technique is to use the assumptions concerned with the property of the acoustic parameter distribution as a prior information. The prior assumptions used in our estimation could be summarized as follows:

Assumption 1: A large part of the model is same medium, so that the majority of the elements in mesh is of the same medium and has the same acoustic parameters.

Assumption 2: Since the inverse problem is ill-conditioned, after one step of Newton-Raphson method coupled with a regularization method is used, the estimated value of the acoustic parameters would be dispersed around the true value.

That is, it is assumed that these two properties are known as a prior information. According to the prior assumptions above, after each iteration of the conventional algorithm is made, a statistical analysis about the estimated acoustic parameters of all elements would be performed. The statistical procedure is as follows:

- 1) Find the maximum and minimum values of the acoustic parameter data ρ_k estimated in the k -th iteration.
- 2) Divide the whole value region ranged from minimum value to maximum value into N equally spaced subregions $\Omega_1, \Omega_2, \dots, \Omega_N$.
- 3) Count the number of estimated data belong to each subregion. (Then, a histogram of the estimated data is obtained.)
- 4) Find the subregion Ω_M with maximum count.
- 5) Examine the number of estimated data in the region including the subregion Ω_M and its neighbor sub-

regions. (The number of subregions in the region are chosen to be 3 or 5. That is, the true value of the acoustic parameter of the main medium will be considered to range in the three subregions $\Omega_{M-1}, \Omega_M, \Omega_{M+1}$ or five subregions $\Omega_{M-2}, \Omega_{M-1}, \Omega_M, \Omega_{M+1}, \Omega_{M+2}$.)

- 6) Modify the estimated values belong to the above subregions to the mean value ρ_{mean} . That is, for the case of three subregions,

$$\rho_k(i) = \begin{cases} \rho_k(i) & \text{if } \rho_k(i) \notin \Omega_{M-1}, \Omega_M, \text{ and } \Omega_{M+1} \\ \rho_{\text{mean}} & \text{if } \rho_k(i) \in \Omega_{M-1}, \Omega_M, \text{ or } \Omega_{M+1}. \end{cases} \quad (20)$$

where \in and \notin mean being in and out of the domain respectively, and ρ_{mean} indicates the arithmetic mean of the estimated data in the subregions Ω_{M-1}, Ω_M and Ω_{M+1} .

After a new estimated values are obtained by the above statistical procedure, the conventional algorithm is again carried out in the next iteration. Thus the conventional algorithm and modification technique based on the statistical analysis are alternatively performed until a “true” acoustic parameter distribution is achieved.

Note that the modification using prior information is only carried out in each iteration process, and is not applied to the final distribution obtained by usual iteration approach. The cost function is not modified by prior information. From the viewpoint of the use of prior information, the approach differs from the Vauhkonen’s approach.

The overall procedure of the reconstruction method can be written as follows:

- step 1:** Give same initial acoustic parameters to all elements as the starting values.
- step 2:** Carry out one step of estimation by the use of Newton-Raphson method coupled with one kind of the regularization method.
- step 3:** Make statistic analysis of the estimated acoustic parameters of all elements, and decide the elements whose acoustic parameters should be corrected. Then correct the estimated parameter values of these elements as their mean value.
- step 4:** Check the convergence of solution. If $(J_{k+1} - J_k)/J_k$ is small enough, then the convergence is reached. If the convergence is not reached, the process jumps to step 2, and the process to follow is repeated until convergence is reached.

4. RECONSTRUCTION RESULTS

While the goal of the sound wave CT is to reconstruct the both distributions of density and sound speed, we confine ourselves to reconstruct the density distribution in this paper due to the difficulty of the whole inverse

problem. The two following reconstruction algorithms are investigated. The first algorithm only uses the Newton-Raphson method coupled with one kind of regularization method under the condition without use of the prior information, i.e., the conventional algorithm. While the second algorithm uses the proposed procedure shown in section 3.2, here, called the proposed algorithm. The number of subregions N is selected as 20 and five subregions Ω_{M-2} , Ω_{M-1} , Ω_M , Ω_{M+1} and Ω_{M+2} are chosen as the region which has a maximum probability to include the true density value of the main medium. Because, the reconstructed result using three subregions, Ω_{M-1} , Ω_M , and Ω_{M+1} , are almost the same as the case of five subregions except that convergence speed is slightly slow.

To compare the reconstruction results of the two algorithms, the reconstruction accuracy E_{sum} is defined as the average relative error of the estimated densities of all elements:

$$E_{sum} = \frac{1}{n} \sum_{j=1}^n \left| \frac{\hat{\rho}_j - \rho_j}{\rho_j} \right| \times 100\% \quad (21)$$

where, $\hat{\rho}_j$ is the estimated density of the j th element, and ρ_j is the true density of the j th element.

4.1. Comparison of the Regularization Methods

During the reconstruction process, the selection of the regularization parameter γ is important. An inappropriate selection can not result in a reasonable reconstruction. Because the selection is related to the drive method, drive frequency, and the size of the FEM mesh, etc, it is a complicated and difficult problem. When the FEM model is driven by a $f = 1,275$ Hz stationary sound wave and the 3-drive mode method described at section 3 is used, the selections of $\gamma = 10^{-24}$ (for TSVD method), $\gamma = 10^{-27}$ (for Tikhonov method) and $\gamma = 10^{-13}$ (for Marquardt method) give relatively better reconstructions respectively. From the reason, these regularization parameters are selected for the comparison of two reconstruction algorithms.

Figures 4–7 indicate the reconstruction results obtained by the conventional algorithm combined with the TSVD and Marquardt regularization methods respectively. The

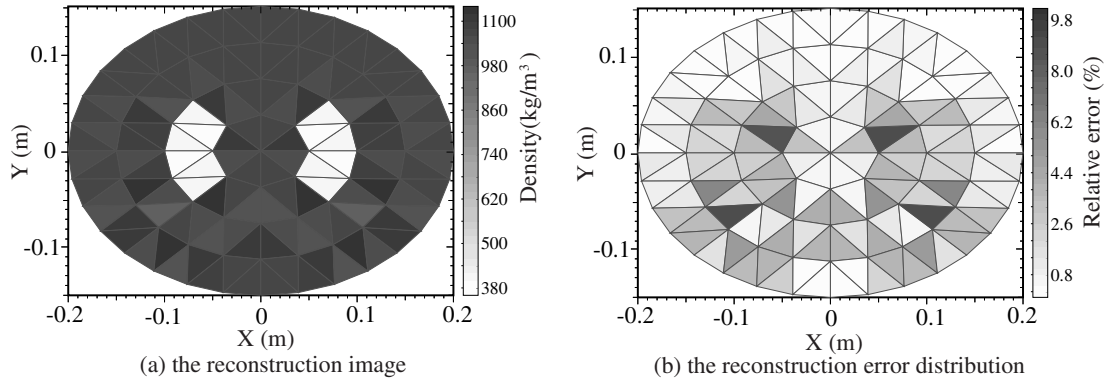


Fig. 4 Reconstruction image and image of the relative errors obtained by the conventional algorithm (TSVD method, $f = 1,275$ Hz, $\gamma = 10^{-24}$). The shaded and light parts indicate the magnitudes of the estimated density and its relative error.

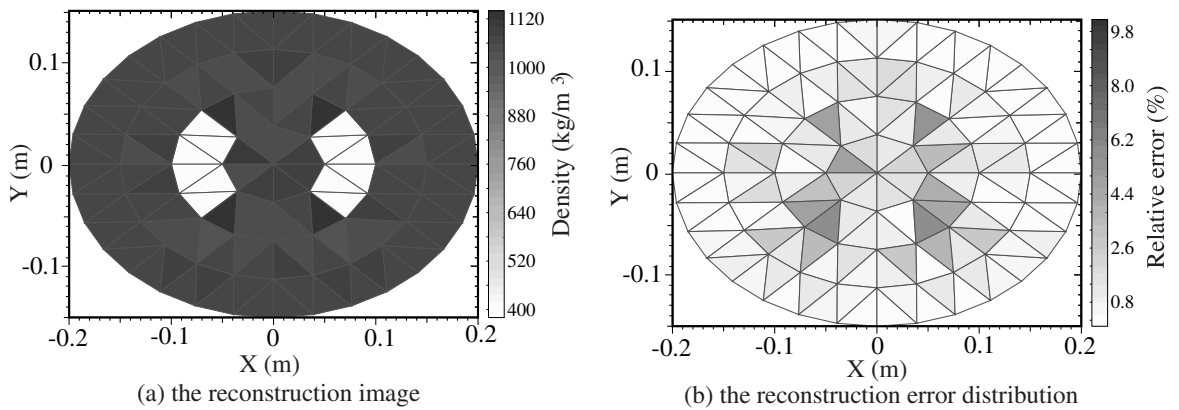


Fig. 5 Reconstruction image and the image of the relative errors obtained by the conventional algorithm (Marquardt method, $f = 1,275$ Hz, $\gamma = 10^{-13}$).

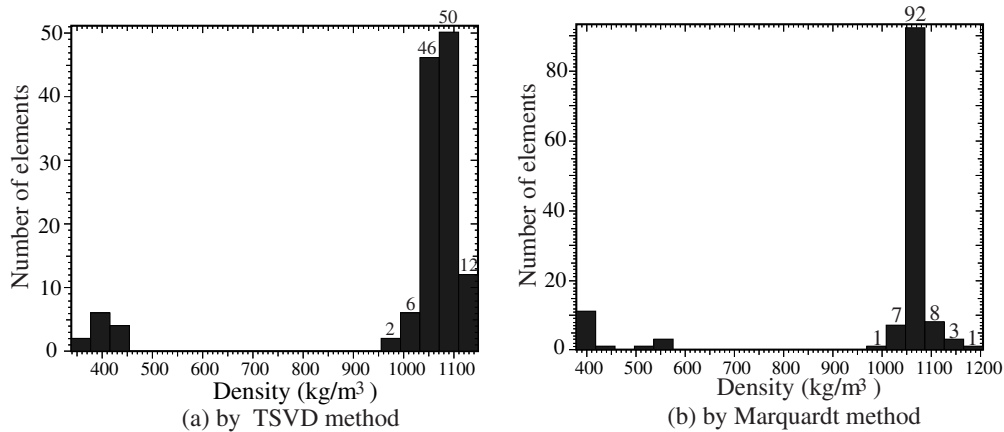


Fig. 6 Histograms of the estimated density obtained by the conventional algorithms. In this case, 20 subregions are selected for making the histogram. The number shown in the figure indicates the number of elements in some subregions.

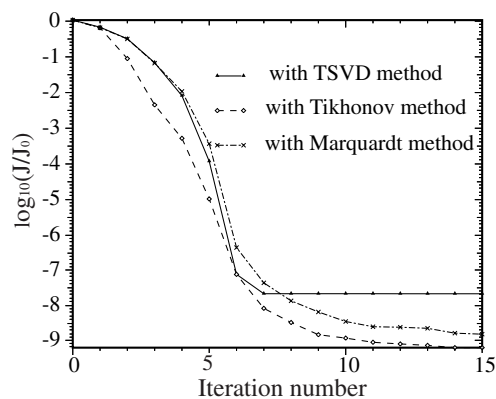


Fig. 7 Convergence curve of the cost function obtained by the conventional algorithm. J_0 indicates the starting value of the cost function.

true density distribution is identical to that shown in Fig. 1 and their initial assumed values are selected as 1,020.0 m/s² for all elements.

These results show that the conventional algorithm using TSVD and Marquardt regularization method can not reach a satisfactory result. It is also found that the results by the use of Tikhonov method gives almost the same reconstruction accuracy.

Figures 8–10 indicate the reconstruction results by the proposed algorithm combined with Marquardt regularization method. The use of TSVD method and Tikhonov method give almost the same reconstruction accuracy as the case of Marquardt method. The initial values are also selected as 1,020.0 m/s² for all elements.

These results show that the proposed algorithm can approach a very accurate reconstruction compared with the conventional algorithm. Table 1 shows the E_{sum} obtained by two algorithms.

Figure 11 shows the comparison of E_{sum} 's convergence for two algorithms. In this case, the result using

Marquardt method is only shown. However, it is found that the convergence obtained by using TSVD and Tikhonov method have almost the same degree of that of Marquardt method.

According to the Fig. 11 and Table 1, the proposed algorithm not only can converge to a less E_{sum} quantity, i.e., more accurate reconstruction, but also has same convergence speed approximately with the conventional algorithm. It is evident that the iterative schemes of the proposed algorithm successfully avoid from being trapped in local minima of the cost function by using the prior information. Although the prior assumption here has certain limitation for other cases, one can make a corresponding assumption according to the concrete situation. However, a proper modification in iterative schemes can always improve the estimate result.

It can also be seen that both the algorithms have a relative greater errors in the white region of the model than in the black region. We believe that it is due to the greater wave number (the ratio of element length to wavelength) in this white part of the ellipse model.

4.2. Effect of the Drive Method

As the multi-drive mode is selected, the question that how many number of drives and how combination of the drives can give a better reconstruction should be investigated. To do it, the drives shown in Fig. 12 are taken into consideration. Four continuous element laterals are driven in each drive and the sound pressures are measured on the rest boundary nodes.

The drives a, b, c, d are selected to be with a clockwise sequence and 45° interval, while the drives e, f, g, h are selected to be with a left-right-up-down sequence. Table 2 shows the reconstruction results of different combinations of drive a, b, c, d, while Table 3 shows the results of different combinations of drive e, f, g, h. These are

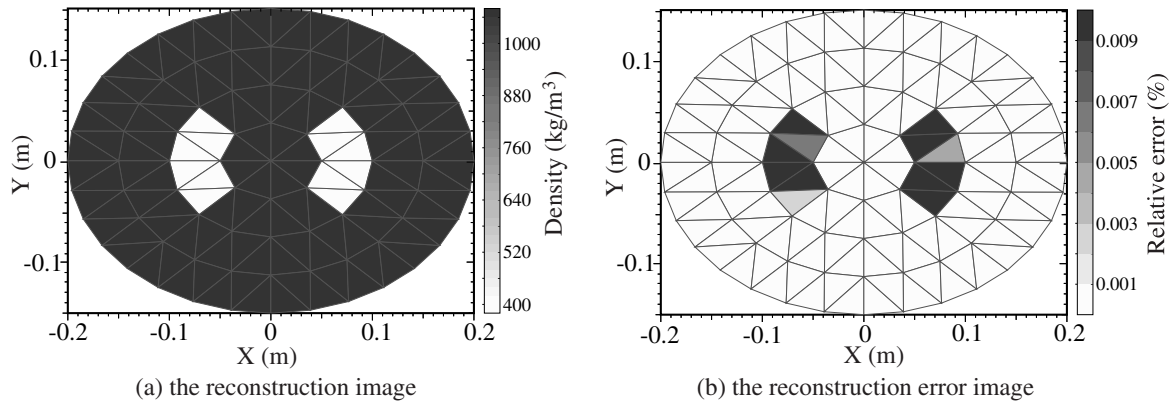


Fig. 8 Reconstruction image and image of the relative errors obtained by the proposed algorithm (Marquardt method, $f = 1,275$ Hz, $\gamma = 10^{-13}$).

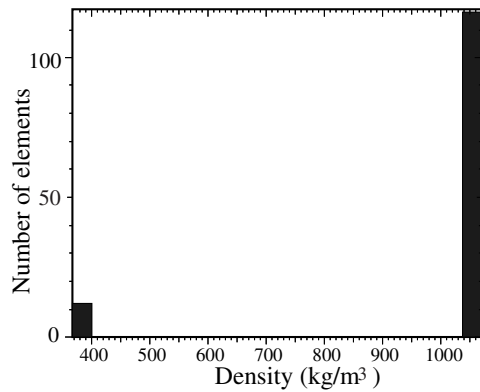


Fig. 9 Histogram of the estimated density obtained by the proposed algorithm coupled with Marquardt method. The uses of TSVD and Tikhonov methods give almost the same histogram.

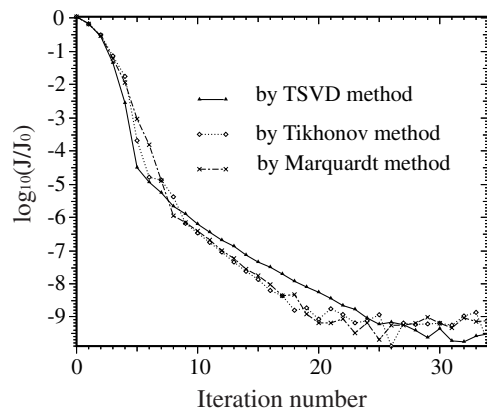


Fig. 10 Convergence curve of the cost function obtained by the proposed algorithm.

Table 1 Comparison of E_{sum} obtained by two algorithms.

Regularization method	TSVD	Tikhonov	Marquardt
By the conventional	2.069%	1.347%	1.071%
By the proposed	0.0043%	0.0086%	0.00375%

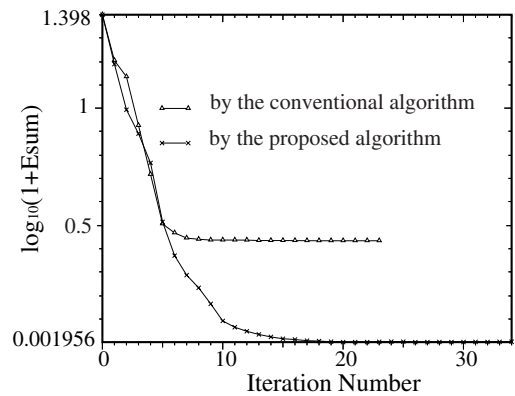


Fig. 11 Comparison of E_{sum} for the conventional and the proposed algorithms. Marquardt method is used as a coupled regularization method in both algorithms.

Table 2 Comparison of E_{sum} obtained by the clockwise direction drive mode.

Mode number (drive combination)	1 (a)	2 (a, b)	3 (a, b, c)	4 (a, b, c, d)
By the conventional	13.0%	7.50%	3.49%	3.25%
By the proposed	10.07%	5.96%	0.3038%	0.99%

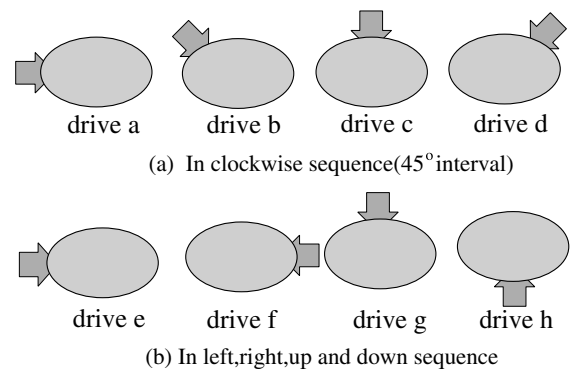


Fig. 12 Illustrations of different drive directions and position.

Table 3 Comparison of E_{sum} obtained by the left, right, up, down direction drive modes.

Mode number (drive combination)	5 (e)	6 (e, f)	7 (e, f, g)	8 (e, f, g, h)
By the conventional	13.0%	3.76%	2.07%	2.67%
By the proposed	10.07%	0.011%	0.001%	0.001%

obtained by using the TSVD regularization method.

From the results of Tables 2 and 3, it can be found that the combination of drive e, f, g, h gives a better reconstruction result than the combination of drive a, b, c, d although the same number of drives, and these drives would be enough to reconstruct. Therefore, a proper choice of the drive method is very important for the reconstruction. It can also be found that the proposed algorithm gives a better result than the conventional algorithm.

4.3. Effect of the Driving Frequency

The reconstruction results (E_{sum}) of different driving frequencies are shown in Fig. 13. In this case the TSVD regularization method is also used. Figure 13 shows that the reconstruction becomes unstable numerically when the frequency get greater than a special value (in our case, 1,575 Hz). It is considered to be relative to the use of the finite element method, because at this time, the ratio of the element length to the sound wavelength in the white part of the ellipse model will be greater than 0.1. Besides, from the Fig. 13, it can be seen that the proposed algorithm shows a better characteristic related to different frequency than the conventional algorithm does again.

4.4. Effect of Measurement Accuracy

Measurement error or noise contamination is inevitable in actual situation. The effects of the measurement accuracy in the two algorithms are also investigated by simulation. In Table 4, the results obtained by drive mode

Table 4 E_{sum} corresponding to different accuracies of measurement data.

Significant digit figures	By conventional algorithm	By proposed algorithm
7 digit	1.99%	0.0062%
6 digit	2.00%	0.029%
5 digit	2.86%	0.110%
4 digit	20.9%	0.393%
3 digit	50.3%	1.366%

7 shown in Table 3 (in left, right, up, down sequence) are shown, where the measurement accuracy is indicated by the significant digit figure. These digit figures mean that the maximum value of the sound pressure (as an input data of inverse problem) has corresponding significant digits. That is, to simulate the measurement error, the input data was truncated at a certain level. Table 4 shows that the measurement accuracy will affect the reconstruction accuracy. It is also found that, for the conventional algorithm, 5 significant digit or more accurate measurement is necessary, while for the proposed algorithm the condition can be relatively loosen. Therefore, the proposed algorithm has a robust characteristic with respect to the measurement accuracy.

4.5. Effect of the Initial Value

The initial acoustic parameter value of each element can be given approximately according to the prior knowledge about the object. However, it is considered that an inappropriate initial assumption deteriorate the convergence and the reconstruction can not approach to a reasonable result. The effect of the initial value on the reconstruction is investigated as shown in Table 5, where $f = 1,275$ Hz and the drive mode 7 is employed.

From the Table, it can be found that the effect of the initial value on the reconstruction result is not great. Comparing with the conventional algorithm, the proposed method is more insensitive to the variation of the initial value.

4.6. On the Case of Asymmetrical Distribution

Because that the estimated acoustic parameters of each element is assumed as a independent variable, the two algorithms do not limit to the symmetric distribution. To confirm it, the distribution shown in Fig. 14 is selected to be reconstructed. The values of the medium density and sound speed in white part, black part and outside of the ellipse model are identical to those of Fig. 1. The reconstruction result is shown in Table 6 and the reconstruction image for two algorithms with the Marquardt regularization method are shown in Fig. 15.

It is found that although the conventional algorithm get worse on the case of asymmetrical distribution, the

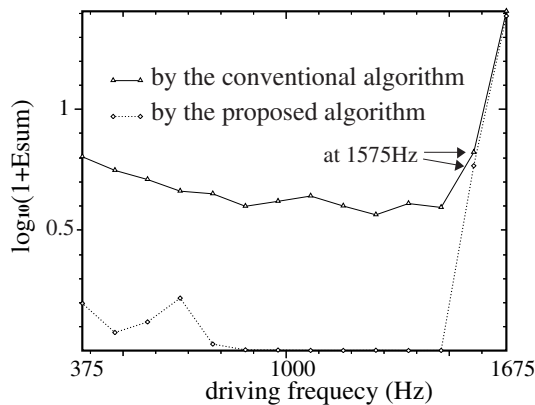
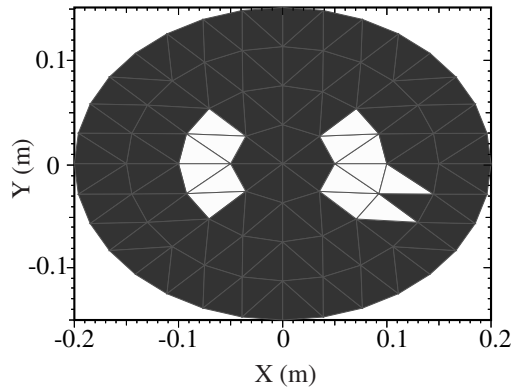
**Fig. 13** Reconstruction errors due to the different driving frequencies.

Table 5 *Esum* corresponding to different initial values (Marquardt regularization method is used).

The initial value (kg/m ³)	800	850	900	1,000	1,050	1,100	1,150
By the conventional	2.569%	2.159%	1.833%	1.049%	1.030%	1.355%	1.896%
By the proposed	0.002%	0.001%	0.001%	0.002%	0.003%	0.001%	0.003%

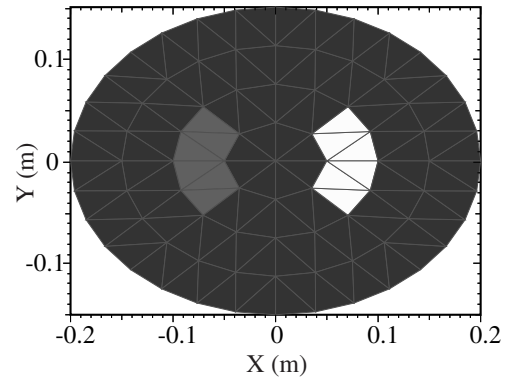
**Fig. 14** Asymmetrical distribution model. The white and black parts indicate the image view of the acoustic parameter distribution.**Table 6** *Esum* corresponding to asymmetrical distribution.

Regularization method	TSVD	Tikhonov	Marquardt
By the conventional	3.908%	2.292%	1.884%
By the proposed	0.009%	0.004%	0.003%

proposed algorithm can still approach a good reconstruction.

4.7. On the Case of Three Kinds of Media

An assumed distribution shown in Fig. 16 is selected to investigate the characteristic when the distribution to be reconstructed has many kinds of media. The grey part in the ellipse model has a acoustic parameter of fat, other part

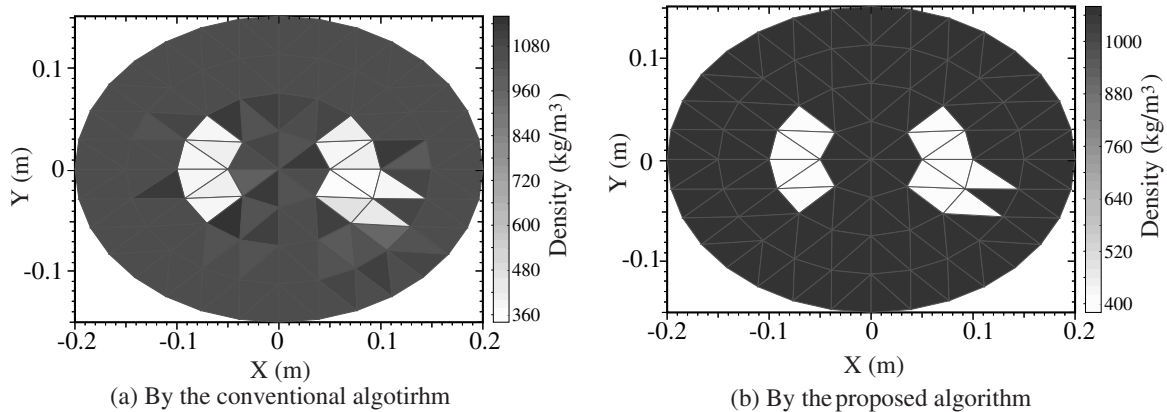
**Fig. 16** Three medium model. The values of density and sound speed in each region are assumed to be: $\rho_1 = 400.0$ kg/m³, $c_1 = 658$ m/s in white region, $\rho_2 = 937.0$ kg/m³, $c_2 = 1,479.0$ m/s in grey region, $\rho_3 = 1,070.0$ kg/m³, $c_3 = 1,566.0$ m/s in black region and $\rho_4 = 1.2$ kg/m³, $c_4 = 340$ m/s in air region.

in Fig. 16 have same medium density and sound speed with Fig. 1. The reconstruction results are shown in Fig. 17 and Table 7.

Results shows that even if the object consist of three kinds of media, the proposed algorithm can approach a good reconstruction.

5. CONCLUDING REMARKS

By incorporating successfully the prior information into the algorithm to reconstruct the density distribution of an object, we investigated the long wavelength sound wave CT technique by numerical simulation. The results are very exciting. The proposed algorithm can reconstruct the density distribution accurately when the input data has no

**Fig. 15** Reconstruction images for asymmetrical case. ($\gamma = 10^{-13}$, $f = 1,275$ Hz, the drive mode 7 is used).

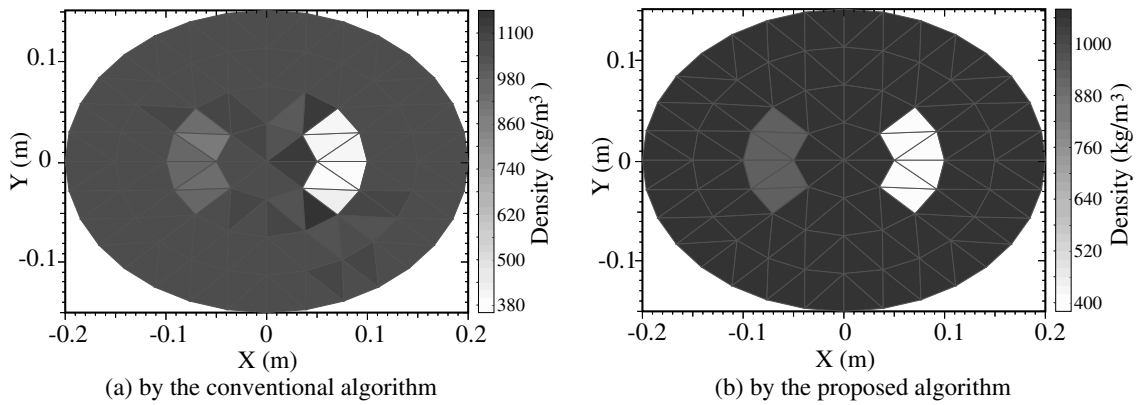


Fig. 17 Reconstruction images (by Marquardt regularization method, $\gamma = 10^{-13}$, $f = 1,275$ Hz, and the drive mode 7 is used).

Table 7 *Esum* corresponding to three kinds of media.

Regularization method	TSVD	Tikhonov	Marquardt
By the conventional	1.574%	1.188%	0.961%
By proposed	0.011%	0.007%	0.005%

measurement errors, and it can also give a relatively satisfactory reconstruction even when the input data has relatively smaller measurement errors. From simulation, some qualitative results about the CT technique, such as how to carry out the drive and the measurement, how many great the frequency should be, and how the measurement accuracy should be, etc. have been obtained. This is important for continuing the research on the CT technique.

For the practical application, the assumption 1 shown in section 3.2 may be not suitable for the complex biological tissue, but we think that, based on the same idea with the proposed algorithm, a similar reconstruction technique is applicable. In the next work, we will improve the space resolution of the reconstruction and study on the reconstruction of that sound speed distribution and the density distribution are unknown.

REFERENCES

- [1] T. Murai and Y. Kagawa, "Numerical simulation of object identification with acoustic scattered waves of long wavelength", *J. Acoust. Soc. Jpn. (J)*, **46**, 905 (1990).
- [2] Y. Kagawa, "Some experimental considerations on ultrasonic computed tomography—Back projection and diffraction algorithm", *J. Acoust. Soc. Jpn. (J)*, **52**, 605 (1996).
- [3] P. M. Meaney, K. D. Paulsen, A. Hartov and R. K. Crane, "Microwave imaging for tissue assessment: Initial evaluation in multitarget tissue-equivalent phantoms", *IEEE Trans. Biomed. Eng.*, **43**, 878 (1996).
- [4] S. Y. Semenov, A. E. Bulyshev, A. E. Souvorov, R. H. Svenson, Y. E. Sizov, V. Y. Borisov, V. G. Posukh, I. M. Kozlov, A. G. Nazarov and G. P. Tatsis, "Microwave tomography: Theoretical and experimental investigation of the iteration reconstruction algorithm", *IEEE Trans. Micro-wave Theory Tech.*, **46**, 133 (1998).
- [5] E. Skudrzyk, *The Foundations of Acoustics* (Springer-Verlag, New York, 1971).
- [6] T. Yamabuchi and Y. Kagawa, "Finite element approach to unbounded Poisson and Helmholtz problems using hybrid-type infinite element", *Trans. IEICE*, **J68-A**, 239 (1985).
- [7] T. Murai, "Electrical impedance computed tomography based on finite element model", *IEEE Trans. Biomed. Eng.*, **BME-32**, 177 (1985).
- [8] M. R. Jones, Y. Yamada and A. Tezuka, "Simulation of optical tomography by an inversion method", *Nippon Kikai Gakkai Ronbunshu Part a*, **62**, 842 (1996).
- [9] T. J. Yorkey, "Comparing reconstruction algorithms for electrical impedance tomography", *IEEE Trans. Biomed. Eng.*, **BME-34**, 843 (1987).
- [10] Y. Bard, "Comparison of gradient methods for the solution of nonlinear parameter estimation problems", *SIAM J. Numer. Anal.*, **7**, 156 (1970).
- [11] P. Hua, J. G. Webster and W. J. Tompkins, "A regularized electrical impedance tomography reconstruction algorithm", *Clin. Phys. Physiol. Meas.*, **9**, Suppl. A, 137 (1988).
- [12] C. D. David and S. Fadil, "An image-enhancement technique for electrical impedance tomography", *Inverse Problems*, **10**, 317 (1994).
- [13] M. Vauhkonen, J. P. Kaipio, E. Somersalo and P. A. Karjalainen, "Electrical impedance tomography with basis constraints", *Inverse Problems*, **13**, 523 (1997).
- [14] M. Vauhkonen and D. Vadasz, "Tikhonov regularization and prior information in electrical impedance tomography", *IEEE Trans. Med. Imag.*, **17**, 285 (1998).



Juzhong Dong was born in Shanxi province, China, in 1964. He received B.E. in automatic control from Xi'an Jiaotong University, Xi'an, China, in 1984 and M.S. degree in underwater acoustic engineering from the Northwestern Polytechnical University, Xi'an, China, in 1987. From 1998 to 2001, he studied for his Ph.D. degree in Faculty of Engineering in Toyama University, Japan. His research interests include electrical acoustics and inverse problem solving.



Yuukou Horita received the B.E., M.E. and Dr. Eng. degree in Electrical and Electronic Engineering from Nagaoka University of Technology, Nagaoka, Japan, in 1984, 1986 and 1995, respectively. In 1995 he joined the Department of Electronics and Computer Science, Faculty of Engineering, Toyama University, Toyama, where he is an Associate Professor. He is engaged in research on

objective quality estimation of coded picture, computer vision and image processing.



Tadakuni Murai was born in Kanazawa, Japan in 1944. He received the B.Sc degree from Toyama University, in 1967, and received the Dr. Eng. Degree from Hokkaido University in 1986. He is now a professor of Dept. of Electrical and Electronic Engineering of Toyama University. His current research interest lies in the field of the numerical approach to various engineering problems, in particular inverse

problem.